

Article

The Effect of Mg Adding Order on the Liquid Structure and Solidified Microstructure of the Al-Si-Mg-P Alloy: An Experiment and *ab Initio* Study

Xiangzhen Zhu, Wei Jiang, Mingrui Li, Huan Qiao, Yuying Wu, Jingyu Qin * and Xiangfa Liu *

Key Laboratory for Liquid-Solid Structural Evolution and Processing of Materials,
Ministry of Education, Shandong University, 17923 Jingshi Road, Jinan 250061, China;
E-Mails: zhuxiangzhen8705@163.com (X.Z.); jiangwei0806@126.com (W.J.);
miraclelisdu@sina.com (M.L.); qiaohuan1124@126.com (H.Q.); wuyuying@sdu.edu.cn (Y.W.)

* Authors to whom correspondence should be addressed;
E-Mails: qin jy@sdu.edu.cn (J.Q.); xfliu@sdu.edu.cn (X.L.);
Tel.: +86-531-8839-2810 (J.Q.); +86-531-8839-2006 (X.L.);
Fax: +86-531-8839-5011 (J.Q.); +86-531-8839-5414 (X.L.).

Academic Editor: Enrique Louis

Received: 1 October 2014 / Accepted: 19 December 2014 / Published: 26 December 2014

Abstract: In this paper, the relationship between the liquid structure and the corresponding solidified microstructure of an Al-Si-Mg-P alloy was studied. Experimental results show that Mg can reduce the phosphorous-modification effect if it was added after adding Al-P alloy. However, when it is added before adding Al-P alloy, Mg has no effect on the phosphorous-modification. It is considered that the difference in liquid structure induced by changing the adding order of Mg should be responsible for the above phenomenon, and was investigated by *ab initio* molecular dynamics simulation (AIMD). It was believed that the high-active Mg atoms could bond P atoms to form P-Mg clusters and then reduce the modification effect of AlP, when pure Mg was added into the prepared Al-Si-P melt. When the pure Mg was added into Al-Si melt before adding Al-P alloy, the Mg atoms would be first occupied by Si atoms to form Mg-Si clusters, and thus lose the ability to eliminate P-Al clusters which dissolve into melt later, leading to a good phosphorous-modification effect.

Keywords: AlP; Mg; modification; Al-Si alloy; liquid structure; evolution; simulation

1. Introduction

The structural relationship between the liquid melt and the corresponding solidified alloy has been a long-standing concern and is not very clear now. In 1927, Levi focused on the correlation between the difference in the liquid melt and its resulting varying performance of solid alloys which have the same composition and underwent the same processing [1]. Since then, many researchers have made attempts to clarify this problem [2–5]. Currently, increasingly strict performance requirements of casting are put forward; therefore, the study of controlling liquid metal state, which is the base to produce an excellent casting, is receiving increasing attention.

Al-Si based alloys are important materials which have been widely used in piston production and other automotive applications. To improve the properties of near-eutectic and hypereutectic Al-Si alloys, it is imperative to modify primary Si grains and add alloying elements. In 1933, researchers found that AlP is a very effective compound to modify primary Si phase [6]. Due to the similar crystal parameters, AlP phase could act as high-efficiency heterogeneous nucleation substrate for the primary Si, resulting in an increase in the number of small Si particles [6–10]. Since then, many modifiers contained P have been invented, such as Cu-P alloy, Si-P alloy and Al-P alloy. Alloying is also an effective method to strengthen the Al-Si based alloys. Mg is an important alloying element to enhance the elevated-temperature properties of Al-Si alloys [11,12]. However, due to its high reactivity, the burning loss of Mg is not a negligible problem. Hence, a secondary addition of Mg is a very common process in casting shop for returning to a normal Mg level. As a high-active element, Mg has the potential to react with P element. This reaction may reduce the modification effect of AlP. However, no study about this problem has been carried out.

In this paper, the fading phosphorous-modification of Si phase induced by changing order of adding Mg and Al-P alloy was revealed by our experiments. To understand the mechanism behind this phenomenon, the liquid structures of the corresponding Al-Si-Mg-P melt and their evolution paths should be investigated. The *ab initio* molecular dynamics simulation (AIMD), which is a computational chemistry method based on quantum chemistry, was adopted to calculate the information of clusters in the Al-Si-Mg-P system.

2. Experimental and Computational Methods

The eutectic Al-12.6Si alloy (all compositions quoted in this work are in wt.% unless otherwise stated) was used to research the effect of adding Mg on the phosphorous-modification of Si phase. The adoptive modifier is Al-3P alloy rod, which was supplied by Shandong Al & Mg Melt Technology Co. Ltd. (Jinan, Shandong, China).

In this study, the Al-12.6Si alloy was remelted in a clay-graphite crucible by an induction furnace. Then, the melt was transferred into a resistance furnace at 780 °C. The following holding process and addition of Mg and Al-P alloy were all operated in the resistance furnace. The addition level of Al-3P alloy (1.0%) and pure Mg (1.5%) is same for two phosphorous-modified samples. The phosphorous-modification parameters are also the same: holding 40 min at 780 °C after adding Al-3P alloy. The only difference in the preparation process is the order of adding Mg. For one Al-12.6Si alloy (marked as “B alloy”), the addition of Mg occurs before adding Al-3P alloy. While for another alloy (marked as “C alloy”),

the addition of Mg occurs after adding Al-3P alloy. The specific operating procedures are shown in Figure 1. The melts were poured into a cast iron mold with a size of 100 mm × 40 mm × 30 mm. The solidification rate of the alloys is about 14 K/s. Specimens with the size of 15 mm × 10 mm × 10 mm were obtained from the center of the entire casting alloys and then mechanically ground and polished using standard routines. The microstructures of the alloys were characterized and analyzed by optical microscope and field emission scanning electron microscope (FESEM, model Hitachi-SU-70, Tokyo, Japan).

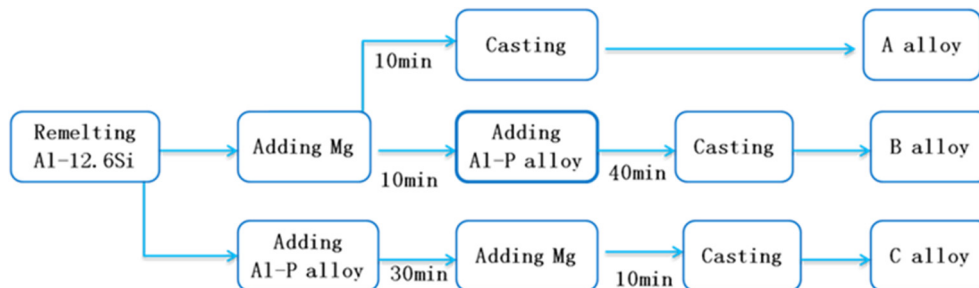


Figure 1. The preparing processes of three samples.

In the experiment, the content of P element in Al-Si melt is only 300 ppm and Mg is 1.5%. As for AIMD, if one kind of atom in an alloy is too small, the statistical error of the structure functions will be large. So, the concentrations of P and Mg were set higher than these in the experimental melt. The AIMD simulations were executed using the Vienna *ab initio* simulation package (VASP) [13] by implementing the projector augmented-wave method [14]. A gradient corrected energy function [15] was adopted. The plane-wave basis set contained components with energies up to 270 eV. Generally, only the Γ -point was used to sample the supercell Brillouin zone. All the simulations were carried out in the canonical ensemble (NVT) through a Nosé [16] thermostat with a characteristic frequency equal to 52 ps⁻¹. Newton's equations of motion were integrated using the Verlet algorithm with a time step of 3 fs. The system of Al₁₇₉Mg₉Si₆P₆ with 200 atoms was equilibrated at $T = 1173$ K (1373 K) for 9 ps with 2000 configurations from the last 6 ps periods being collected for structural analysis.

3. Results and Discussion

Figure 2 shows the microstructures of three Al-12.6Si-1.5Mg alloys. It is clear that the Si phase in the A alloy without P exists in the form of eutectic Si phase, and the Mg₂Si phase also exists in the matrix, as shown in Figure 2a,b. There is no proper Al-Si-Mg diagram that can describe in detail all the phases (containing α -Al, eutectic Mg₂Si, primary Si and eutectic Si) in Al-12.6Si-1.5Mg alloys, but we can speculate on these phases based on the binary Al-Si and Mg-Si diagrams. As it is well known, Al-12.6% Si is just the eutectic Al-Si alloy. However, since part of Si atoms was bonded by Mg atoms to form Mg₂Si phase, the content of Si which would crystallize as Si phase is less than 12.6%. Therefore, the microstructure of Al-12.6Si-1.5Mg alloy possesses the characteristics of hypoeutectic Al-Si alloys, and no primary Si particles were found. While, when Al-P alloy was added into the melt after adding Mg, some small primary Si particles appear, as shown in Figure 2c.

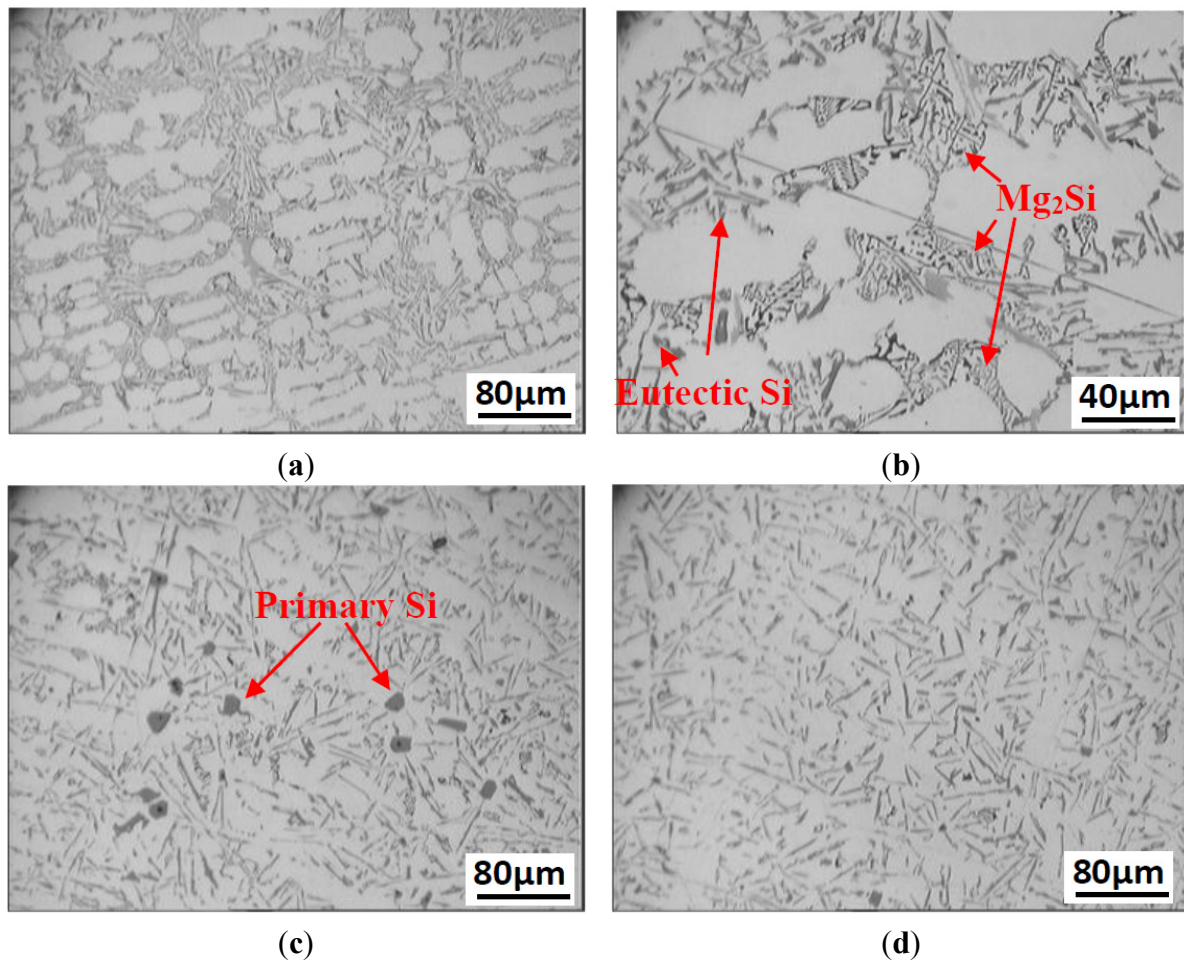


Figure 2. The microstructures of Al-12.6Si-1.5Mg alloys: (a,b) A alloy; (c) B alloy with some primary Si grains, into which Al-P alloy was added after adding Mg; (d) C alloy with few primary Si grains, into which Al-P alloy was added before adding Mg.

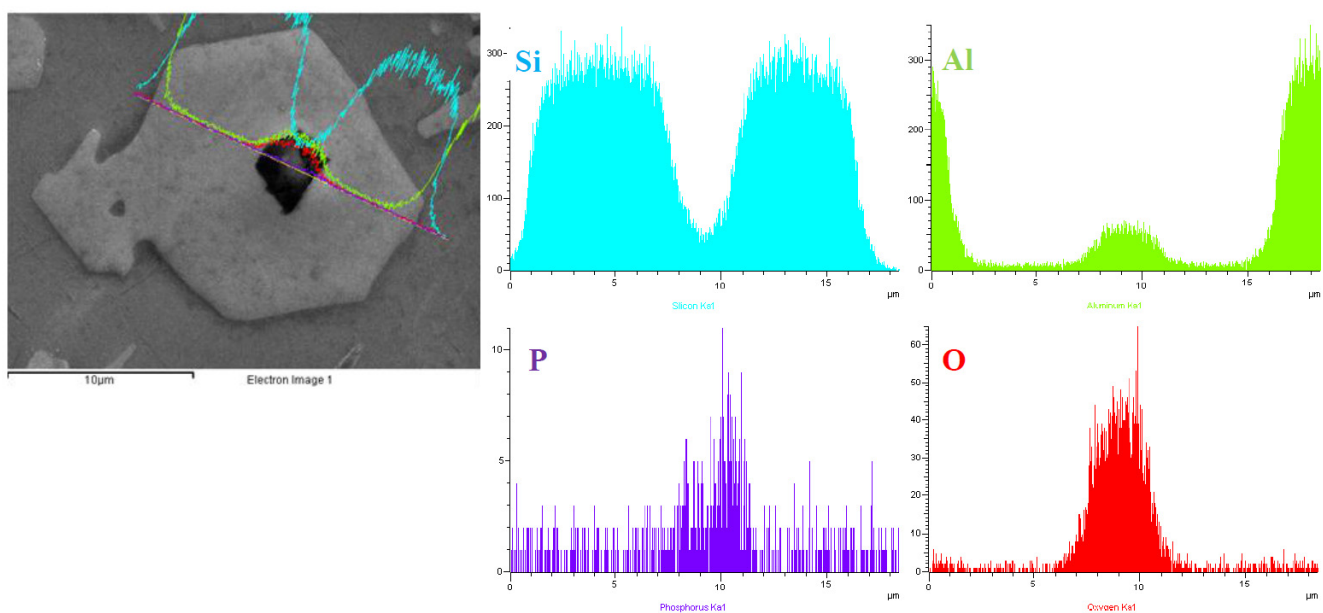


Figure 3. The EDS analysis of the black phase in the center of a primary Si particle. The black phase contains Al, P and O, and is considered as AlP.

Figure 3 shows the EDS analysis of a typical primary Si particle. It was found that a black phase exists in the center of primary Si phase, and is rich in Al, P and O elements. It is considered that this black phase is AlP, and the existence of O element is due to the oxidation and hydrolysis of AlP during specimen preparation [7]. AlP phase and Si phase have the same face-centered cubic (fcc) crystal structure and very similar lattice parameters ($a_{\text{AlP}} = 5.45 \text{ \AA}$, $a_{\text{Si}} = 5.42 \text{ \AA}$), as shown in Figure 4. So, AlP can act as the highly effective heterogeneous nucleation substrate for primary Si phase. Due to the existence of AlP, many Si atoms in this eutectic melt could be absorbed and bonded by AlP during solidification, and then precipitated as primary Si phase, rather than eutectic Si phase. This transformation from the eutectic Si phase to the primary Si phase is the aim of the phosphorous-modification.

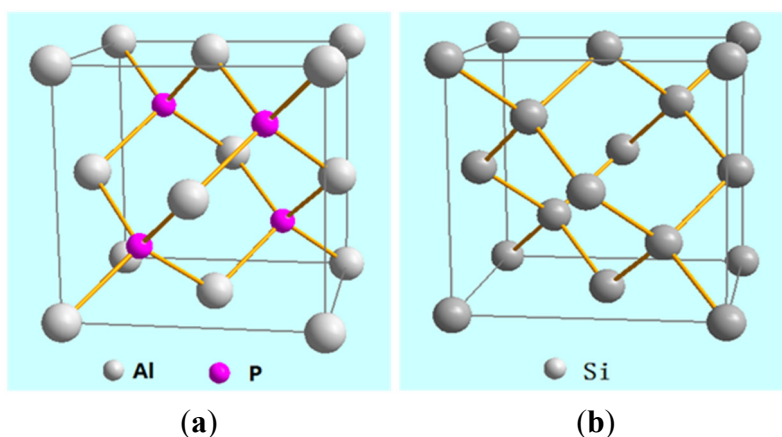


Figure 4. The crystal structures of (a) AlP; (b) Si. They both have face-centered cubic structure, and $a_{\text{AlP}} = 5.45 \text{ \AA}$, $a_{\text{Si}} = 5.42 \text{ \AA}$.

Figure 2d displays the microstructure of C alloy. Though the C alloy was also supplied with Al-3P alloy, it has few primary Si particles. It indicates the AlP did not play its role of heterogeneous nucleation substrate. Compared with B alloy, the only difference in the preparation process is the order of adding Mg element. It is supposed that Mg plays a pivotal role in reducing the modification effect of AlP.

It is well known that the liquid metal is the source of casting, and the solid microstructure originates from the liquid structure. The liquid structure of the Al-Si-Mg-P alloy was analyzed using AIMD simulations to investigate the solidification mechanisms caused by particular Mg alloying orders. As discussed above, it is considered that the reactions related with Mg are the key point. It seems that Mg may react with AlP, according to our experimental results. In general, Mg tends to strongly react with the Si element to form Mg_2Si . Hence, the competition between the above two reactions should be investigated, and the affinities of P-Mg and Si-Mg were analysed in this study. For the convenience of comparing these two affinities, the atomic percents of Si and P were all set to the same value (3%). The atomic percent of Mg was set as 4.5%. So, the ration of Mg to P is just that in Mg_3P_2 compound, and the ration of Mg to Si is less than that in Mg_2Si compound. In other words, the content of Si is in excess, which could enhance the affinity of Si-Mg and is a little similar with the conditions in the experimental melt.

Figure 5 shows the partial correlation functions (PCFs) of $\text{Al}_{179}\text{Mg}_9\text{Si}_6\text{P}_6$ alloy at 1173 K. In order to describe the liquid structure of this Al-Si-Mg-P alloy comprehensively, there needs to be 10 PCFs, namely, $g_{\text{PAl}}(r)$, $g_{\text{PMg}}(r)$, $g_{\text{PSi}}(r)$, $g_{\text{PP}}(r)$, $g_{\text{MgAl}}(r)$, $g_{\text{MgMg}}(r)$, $g_{\text{MgSi}}(r)$, $g_{\text{SiAl}}(r)$, $g_{\text{SiSi}}(r)$ and $g_{\text{AlAl}}(r)$. Since the

$g_{AlAl}(r)$ is rather normal, we only present the other nine PCFs in this investigation. To facilitate the comparison and analysis, three figures, which are related with P, Mg and Si, respectively, are used to show these nine PCFs.

Four P-related $g(r)$ curves are plotted in Figure 5a. It is observed clearly that the first peak of the $g_{PMg}(r)$ curve is much higher than those of other three P-related $g(r)$ curves, indicating that the affinity of P-Mg pairs is strongest. The P-Al pairs have a second strong affinity. Now, we tend to $g_{PSi}(r)$ and $g_{PP}(r)$ curves. Since the second peak of $g_{PSi}(r)$ curve is more obvious than the first peak, the Si atoms tend to exist at the second coordination shell rather than at the first coordination shell of P atoms, avoiding meet P atoms directly. The atomic radius of P atom is 0.11 nm. So, if there were P-P pairs, a pronounced first peak should be at 0.22 nm. However, the $g_{PP}(r)$ curve in Figure 1a does not demonstrate the first peak at 0.22 nm, meaning the P-P pairs are extremely scarce. The structural information from $g_{PSi}(r)$ and $g_{PP}(r)$ curves is in good accordance with our previous study [17]. On the basis of above analysis, it can be concluded that P atoms tend to combine with Mg atoms preferentially and then with Al atoms, but would not bond with Si atoms or other P atoms. It also can be shown that Mg element has the potential to eliminate P-Al clusters and reduce the modification effect of AIP.

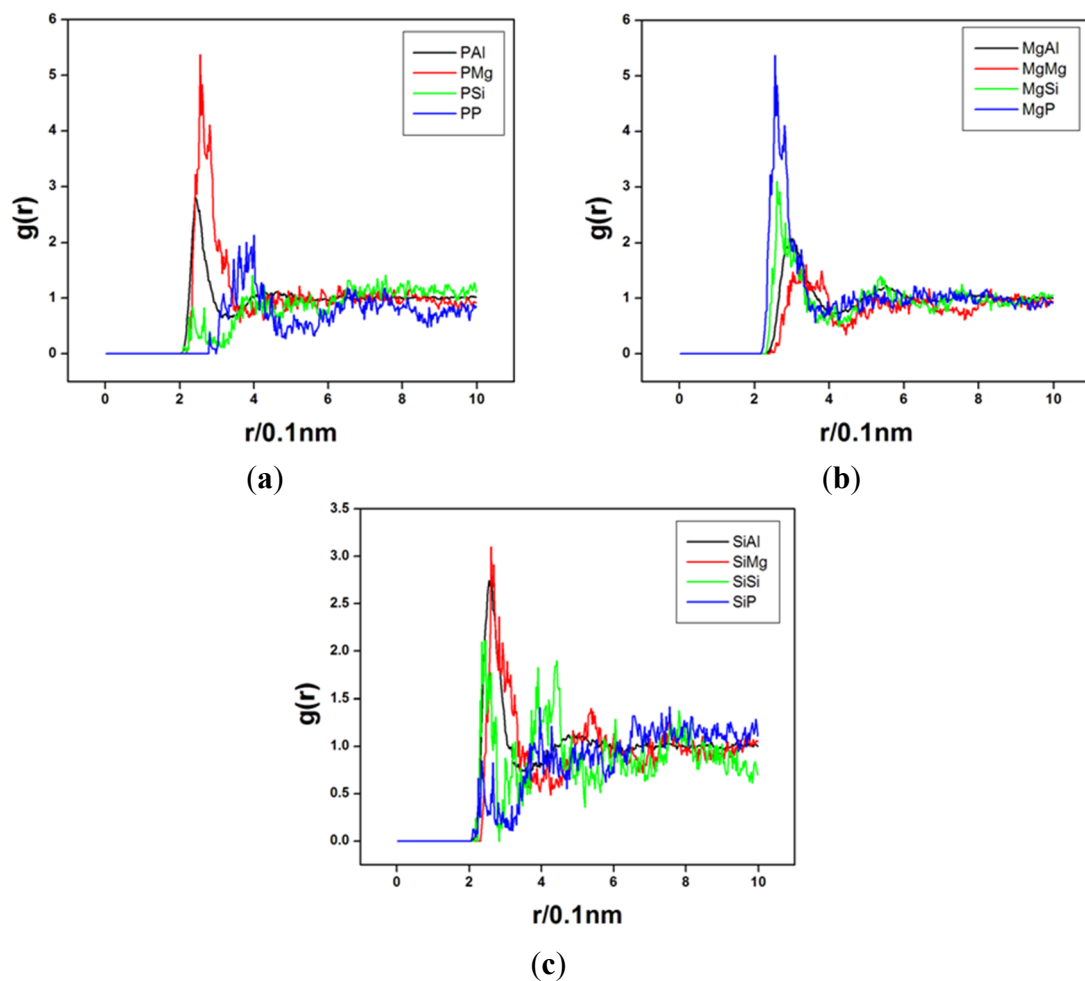


Figure 5. The partial pair correlation functions of $\text{Al}_{179}\text{Mg}_9\text{Si}_6\text{P}_6$ system at 1173K. (a) $g(r)$ curves related with P element; (b) $g(r)$ curves related with Mg element; (c) $g(r)$ curves related with Si element. The $g(r)$ curves show that the affinity of P-Mg is strongest, followed by Mg-Si and P-Al.

The chemical environment around P atoms is shown in Table 1. In the table, N_{ij} is the partial coordination number around a P atom, R_{ij} is the percentage of element i in the partial coordination number of element j . The parameter D_{ij} is the deviation degree between R_{ij} and its nominal value (random distribution), reflecting the chemical short-range order (CSRO) around P atoms. D_{ij} is defined as:

$$D_{ij} = (R_{ij} - \text{Nominal}) / \text{Nominal} \times 100\% \quad (1)$$

Table 1. Chemical environment around P atoms.

Terms	N_{ij}		R_{ij} (%)		Nominal	D_{ij} (%)	
	1173 K	1373 K	1173 K	1373 K		1173 K	1373 K
PAI	5.91	5.95	88.70	92.15	89.50	−0.89	2.96
PMg	0.72	0.46	10.75	7.16	4.50	138.89	59.11
PSi	0.04	0.05	0.54	0.69	3.00	−82.00	−77.00
PP	0.00	0.00	0.00	0.00	3.00	−100	−100

Both at 1373 K and 1173 K, the partial coordination numbers of Al atoms around P atoms (5.95 and 5.91, respectively) are very close to 6, which is similar with that in the Al-Si-P system [17]. While, the number of Mg atoms in the first coordination shell is less than 1. It should be noted the number of Al atoms is high, mainly because the solvent Al atoms are extremely plentiful in this Al-rich melt, and not because the P-Al cluster is the strongest cluster. To measure the strength or importance of the clusters, R_{ij} and D_{ij} should be investigated.

At 1373 K, the R_{PAI} (92.15) and R_{PMg} (7.16) are all greater than their nominal values (89.50 and 4.50). However, the D_{PAI} is only 2.96, meaning that the Al content in the first coordination shell of P atoms is just a little higher than the nominal value (random distribution). In other words, P-Al cluster is not a very strong cluster in this system. For P-Mg pairs, the value of D_{PMg} is up to 59.11. It means P atoms have a higher tendency to combine with Mg atoms.

Moreover, when the temperature is cooled down to 1173 K, the partial coordination number of Mg atoms increases and the value of D_{PMg} reaches 138.89. While, the three parameters of P-Al pairs (N_{PAI} , R_{PAI} and D_{PAI}) all reduce as the temperature drops. These changes of parameters indicate that the P-Mg cluster would be enhanced and P-Al cluster would be weakened during the solidification process. What should be paid particular attention is that the D_{PAI} is −0.89. This negative value is of much significance: when the temperature is below 1173 K, the CSRO between P atoms and Al atoms is very weak, and the P-Mg cluster is the most pronounced cluster in this alloy.

The structural information of P-Si pairs and P-P pairs is also shown in Table 1. The parameters N_{PSi} , which are only 0.05 at 1373 K and 0.04 at 1173 K, demonstrate that the partial coordination number of Si atoms is very little, and becomes lower as the temperature decreases. As for P-P pairs, the N_{PP} value of 0 and D_{PP} value of −100 declare that in fact there are no P-P pairs in the melt.

Now, based on the above integrated information from the $g(r)$ curves and chemical environment, the behavior rule of P atoms is revealed. When P atoms enter the melt, they react with Mg atoms preferentially, followed by Al atoms. Furthermore, P atoms do not combine with Si atoms and other P atoms.

According to the behavior rule of P atoms, it seems that the addition of Mg would eliminate part of P-Al cluster and reduce the modification effect of AlP, according to the conditions of C alloy. However,

when the Mg was added to Al-Si melt before adding Al-P alloy, the modification effect was positive, just as in the case of B alloy. So, the behavior rule of Mg atoms should also be studied carefully.

Figure 5b shows the four Mg-related $g(r)$ curves. It is obvious the first peak of $g_{MgP}(r)$ curve is much higher than those of other three $g(r)$, implying that Mg atoms tend to combine with P atoms, preferentially. It should be known that $g_{ij}(r)$ is equal to $g_{ji}(r)$ in simulation, so $g_{MgP}(r)$ is the same with $g_{PMg}(r)$. The next most important curve is the $g_{MgSi}(r)$ curve, which has the second-ranked peak. Hence, for Mg atoms, it is the second-favorite choice to combine with Si atoms. Then, Al atoms also have a certain degree of potential to bond with Mg atoms, but Mg-Mg pairs are few. The Si-related $g(r)$ curves are also considered, as shown in Figure 5c. With regards to Si atoms, combining with Mg atoms is the preferred choice. It means that the Mg atoms would form Mg-Si clusters in Al-Si melt.

One arbitrary configuration out of 2000 is visualized in Figure 6. By inspection of the visualized configurations, it is found that P atoms tend to be near Mg atoms, and so do Si atoms, agreeing with the information from $g(r)$ curves.

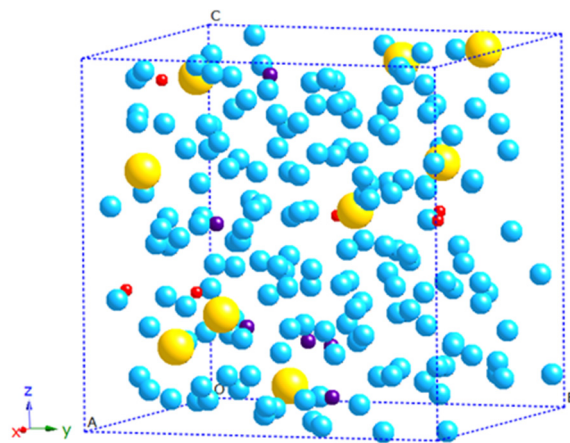


Figure 6. Visualization of an arbitrary configuration of liquid $Al_{179}Mg_9Si_6P_6$ system at 1173 K (Al: blue ball; Mg: yellow ball; Si: violet ball; and P: red ball).

Based on the above analysis, the three strongest clusters are listed as follows: (1) P-Mg cluster > (2) Mg-Si cluster > (3) P-Al cluster.

Among them, the P-Mg cluster is much stronger than the other two clusters. However, the fact that the first peak of $g_{MgSi}(r)$ curve is just a little higher than that of $g_{PAl}(r)$ shows that the Mg-Si cluster is just a little stronger than P-Al cluster in this $Al_{179}Mg_9Si_6P_6$ system.

It should be specially mentioned that the above analysis reflects the conditions of the melt in equilibrium. While, in our experiments, the raw materials are not added to the Al-Si melt at the same time. So, some pre-existing clusters would come into being when the first addition has been completed but the second addition has not been done. Even after the second addition, those pre-existing can also survive for a certain time. They need some time to evolve to equilibrated clusters. However, if the melt was casted before it could reach the balanced or near-balanced state, the survived pre-existing clusters would play a role, making the solid microstructure different from the equilibrated microstructure.

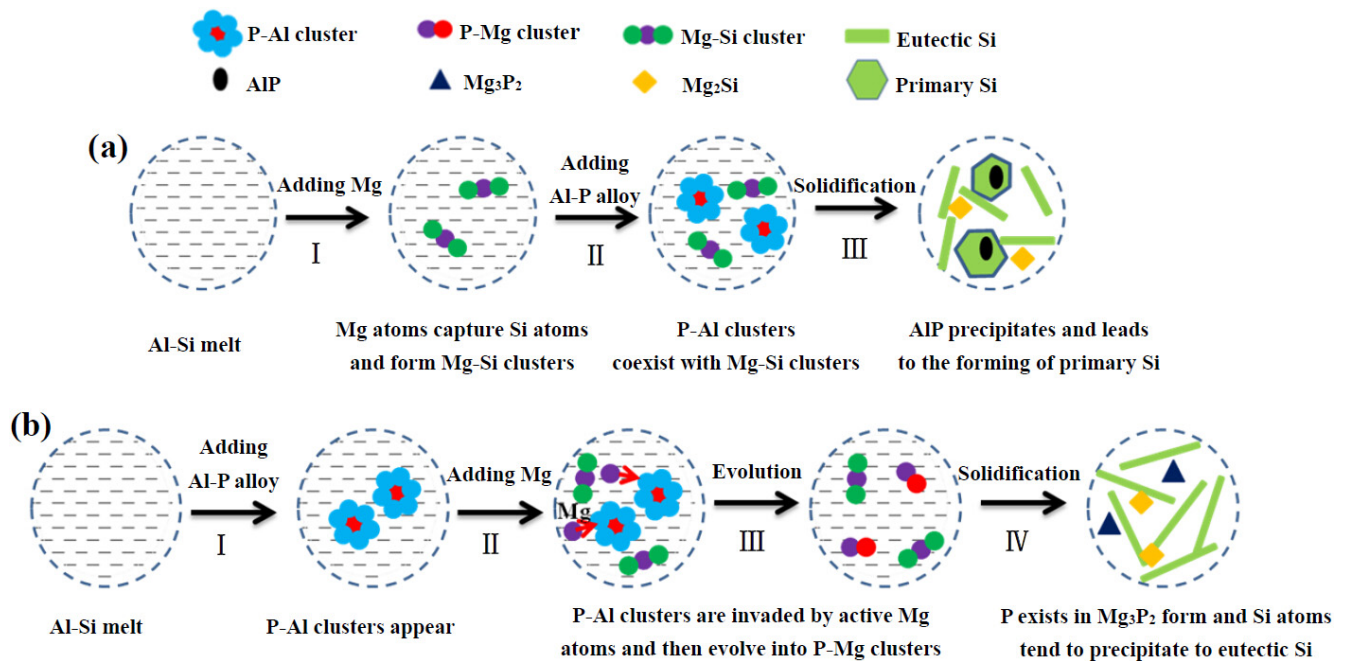


Figure 7. The schematics of the two evolution paths of the Al-Si-Mg-P liquid melt structure induced by changing order of adding Mg and its resulting solidification microstructure. **(a)** when pure Mg was added into Al-Si melt before addition of Al-P alloy, Mg-Si clusters formed firstly and can coexist with P-Al clusters. In the solidification process, the P-Al clusters can precipitate as AIP and then lead to the forming of primary Si; **(b)** when pure was added in to melt after the addition of Al-P alloy, P-Al clusters were invaded by active Mg atoms dissolved from pure Mg and then evolved into P-Mg clusters. In the solidification process, P precipitated as Mg₃P₂, rather than AIP. So, no primary Si particles formed due to the absence of AIP.

Figure 7 depicts the two evolution paths of the Al-Si-Mg-P liquid melt structure induced by implementing different adding orders of Mg. For B alloy, its evolution path is relatively simple and can be divided into three stages, as shown in Figure 7a. In stage I, pure Mg was added into the binary Al-Si melt. In this phosphorous-free melt, the high-active Mg atoms would bond Si atoms and form Mg-Si clusters. The Al-P alloy was added into the melt in the following stage II. Then, AIP compound, which preexists in the Al-P alloy, would dissolve in the melt and evolves into P-Al clusters. That is to say the Mg-Si clusters co-existed with P-Al clusters at the beginning of the stage II. According to the above AIMD results of the melt in equilibrium, the Mg-Si clusters should react with P-Al clusters and evolve to P-Mg clusters. While, considering the experimental result of alloy B, it is speculated that this evolution in the experimental melt could not be finished in a short time: (1) In the experimental Al-12.6Si-1.5Mg-0.03P melt, the amounts of Al atoms and Si atoms are much more than these of Mg atoms and P atoms. So, The P-Al clusters are the P-centered clusters [17], and Mg-Si clusters are the Mg-centered clusters. If P atoms could combine with Mg atoms to form P-Mg clusters, P atoms should get close to and go through the Si atoms zone surrounding the centered Mg atoms in Mg-Si clusters. While, as discussed above, there exists a large tendency to repel each other between P atoms and Si atoms, which blocks the formation of P-Mg clusters. (2) The electronegativity, which was introduced by Pauling in 1932 [18], is a chemical property that describes the tendency of an atom or a

functional group to attract electrons (or electron density) towards itself. The electronegativity difference actually reflects the bonding nature of atomic pairs in alloys. The larger electronegativity difference between constituent elements helps the formation of clusters and compounds [19]. While, according to the electronegativity equalization principle, once Mg atoms combine with Si atoms to form Mg-Si clusters, the electronegativity of Mg would increase, decreasing the electronegativity difference between Mg and P atoms. So, the tendency of Mg to combine P becomes weak. In other words, the Mg atoms in Mg-Si clusters have a lower activity, losing the ability to eliminate P-Al clusters quickly. Therefore, P-Al clusters could coexist with Mg-Si clusters for a long time. However, after only 40 min, the melt was poured into a mould and solidification (stage III) took place. With the decrease in the melt temperature, the co-existing Mg-Si clusters and P-Al clusters grew into crystalline phases correspondingly: Mg_2Si and AlP phases. As the highly effective heterogeneous substrate for primary Si phase, AlP could absorb and bond many Si atoms, and then make them precipitate as primary Si phase, resulting in a microstructure like that of B alloy.

As discussed above, Si plays a suppressive role in the elimination of part of P-Al clusters induced by Mg and ensures a good phosphorous-modification effect (*i.e.*, ensure the transformation from part of eutectic Si plates to some small and distributed primary Si grains), by combining with Mg atoms and reducing the activity of Mg. This phenomenon also appeared in Li's experiment [20]. In his experiment, the prepared Al-20Mg₂Si-3Si alloy could also be modified by AlP. The content of Mg in the prepared Al-20Mg₂Si-3Si alloy is up to 12.7%, but all Mg atoms were bonded with Si atoms and existed in the Mg-Si clusters before adding Al-P alloy. So, Mg had no effect on the phosphorous-modification

As for the C alloy, its evolution path can be divided into four stages, as shown in Figure 7b. The Al-P alloy was added firstly in stage I, resulting in many P-Al clusters appearing in the Al-Si melt. In the next stage II, pure Mg with high activity was added and dissolved into the melt. As discussed above, elemental Mg tends to combine with P atoms preferentially. So, the pre-existing P-Al clusters were invaded by these active Mg atoms and then evolved into P-Mg clusters in a short period of time (stage III). Of course, Mg atoms are excessive, and most of them also combined with Si atoms, forming Mg-Si clusters. The next stage IV is the solidification. P would precipitate in the form of Mg_3P_2 , which could not induce the formation of primary Si. So, the microstructure of C alloy has few primary Si grains.

4. Conclusions

In this paper, the reduction of a phosphorus-modification effect, induced by changing the adding order of Mg and an Al-P alloy, was investigated. The AIMD simulation was used to investigate the liquid structure of Al-Si-Mg-P system to reveal the potential mechanism.

(1) Elemental Mg has the high potential to combine with P atoms. If pure Mg was added into the melt which contains many P atoms, Mg can eliminate P-Al clusters quickly and reduce the phosphorous-modification effect.

(2) Elemental Si can prevent P-Al clusters from the elimination induced by Mg. If the pure Mg was added into Al-Si melt before adding Al-P alloy, Si atoms can combine with Mg atoms and reduce the activity of Mg, then make them lose the ability to eliminate P-Al clusters and ensure a good phosphorous-modification effect.

Acknowledgments

The authors wish to thank the financial support of the National Natural Science Foundation of China (No.50971082), the National Natural Science Foundation of China (No.51001065) and the National Basic Research Program of China (973 Program, No.2012CB825702).

Author Contributions

Xiangzhen Zhu, Jingyu Qin, Yuying Wu and Xiangfa Liu conceived and designed the experiments and simulations; Wei Jiang, Mingrui Li and Huan Qiao performed the experiments; Jingyu Qin performed the simulations; Xiangzhen Zhu, Yuying Wu, Jingyu Qin and Xiangfa Liu analyzed the data; Xiangzhen Zhu wrote the paper.

Conflicts of Interest

The authors declare no conflict of interest.

References

1. Levi, A. Heredity in cast iron. *The Iron Age* **1927**, *6*, 960–965.
2. Frank, F. Supercooling of liquids. *Proc. R. Soc. London Ser. A* **1952**, *215*, 43–46.
3. Vertman, A.; Samarin, A.; Yakobson, A. Structure of liquid eutectics. *Izv. Akad. Nauk SSSR, Otd. Tekhn. Nauk., Met. i Toplivo* **1960**, *3*, 17–21.
4. Li, P.-J.; Zhang, Y.F.; Nikitin, V.; Kandalova, E.; Nikitin, K. Hereditary effect of Al-based modifiers and grain refiners on structure and properties of A356. 2 alloys. *Trans. Nonferrous Met. Soc. China* **2002**, *12*, 233–237.
5. Liu, X.-F.; Bian, X.F.; Qi, X.G.; Ma, J. Structural heredity between Al₅Ti₁B and AlTi, AlB master alloys. *Trans. Nonferrous Met. Soc. China* **1999**, *9*, 806–809.
6. Sterner, R.; Rainer, C. Aluminum silicon alloy with a phosphorus content of 0.001%–0.1%. U.S. Patent 1940922, 26 December 1933.
7. Zhu, X.; Wu, Y.; Li, C.; Li, P.; Qiao, H.; Liu, X. The dispersive orientated-precipitation of AlP on alumina film and its effect on the primary Si gathering behavior in the Al–Si alloy surface layer. *CrystEngComm* **2014**, *16*, 5583–5590.
8. Ho, C.; Cantor, B. Heterogeneous nucleation of solidification of Si in Al–Si and Al–Si–P alloys. *Acta Metall. Mater.* **1995**, *43*, 3231–3246.
9. Faraji, M.; Todd, I.; Jones, H. Effect of solidification cooling rate and phosphorus inoculation on number per unit volume of primary silicon particles in hypereutectic aluminium—Silicon alloys. *J. Mater. Sci.* **2005**, *40*, 6363–6365.
10. Liu, X.; Qiao, J.; Liu, Y.; Li, S.; Bian, X. Modification performance of the Al–P master alloy for eutectic and hypereutectic Al–Si alloys. *Acta Metall. Sin.* **2004**, *40*, 471–476.
11. Samuel, F.H.; Samuel, A.M.; Liu, H. Effect of magnesium content on the ageing behaviour of water-chilled Al–Si–Cu–Mg–Fe–Mn (380) alloy castings. *J. Mater. Sci.* **1995**, *30*, 2531–2540.
12. Caceres, C.H.; Davidson, C.J.; Griffiths, J.R.; Wang, Q.G. The effect of Mg on the microstructure and mechanical behavior of Al–Si–Mg casting alloys. *Metall. Mater. Trans. A* **1999**, *30*, 2611–2618.

13. Kresse, G.; Furthmüller, J. Efficiency of *ab initio* total energy calculations for metals and semiconductors using a plane-wave basis set. *Comput. Mater. Sci.* **1996**, *6*, 15–50.
14. Kresse, G.; Joubert, D. From ultrasoft pseudopotentials to the projector augmented-wave method. *Phys. Rev. B* **1999**, *59*, 1758.
15. Perdew, J.P.; Wang, Y. Pair-distribution function and its coupling-constant average for the spin-polarized electron gas. *Phys. Rev. B* **1992**, *46*, 12947.
16. Nosé, S. A unified formulation of the constant temperature molecular dynamics methods. *J. Chem. Phys.* **1984**, *81*, 511–519.
17. Qin, J.; Zuo, M.; Gu, T.; Liu, X. The featured local structural units in liquid Al₈₀Si₁₅P₅ alloy and their relationship with Si modification. *J. Alloy. Compd.* **2010**, *492*, 525–528.
18. Pauling, L. The nature of the chemical bond. IV. The energy of single bonds and the relative electronegativity of atoms. *J. Am. Chem. Soc.* **1932**, *54*, 3570–3582.
19. Lu, P.; Liu, C.; Dong, D. Effects of atomic bonding nature and size mismatch on thermal stability and glass-forming ability of bulk metallic glasses. *J. Non-Cryst. Solids* **2004**, *341*, 93–100.
20. Li, C.; Liu, X.; Wu, Y. Refinement and modification performance of Al–P master alloy on primary Mg₂Si in Al–Mg–Si alloys. *J. Alloy. Compd.* **2008**, *465*, 145–150.

© 2014 by the authors; licensee MDPI, Basel, Switzerland. This article is an open access article distributed under the terms and conditions of the Creative Commons Attribution license (<http://creativecommons.org/licenses/by/4.0/>).